Accelerating potential of mean force calculations for lipid membrane permeation: System size, reaction coordinate, solute-solute distance, and cutoffs

Naomi Nitschke, Kalina Atkovska, and Jochen S. Hub[a)]
Institute for Microbiology and Genetics, Georg-August-University Göttingen, Justus-von-Liebig-Weg 11, 37077 Göttingen, Germany

(Received 4 August 2016; accepted 9 September 2016; published online 27 September 2016)

Molecular dynamics simulations are capable of predicting the permeability of lipid membranes for drug-like solutes, but the calculations have remained prohibitively expensive for high-throughput studies. Here, we analyze simple measures for accelerating potential of mean force (PMF) calculations of membrane permeation, namely, (i) using smaller simulation systems, (ii) simulating multiple solutes per system, and (iii) using shorter cutoffs for the Lennard-Jones interactions. We find that PMFs for membrane permeation are remarkably robust against alterations of such parameters, suggesting that accurate PMF calculations are possible at strongly reduced computational cost. In addition, we evaluated the influence of the definition of the membrane center of mass (COM), used to define the transmembrane reaction coordinate. Membrane-COM definitions based on all lipid atoms lead to artifacts due to undulations and, consequently, to PMFs dependent on membrane size. In contrast, COM definitions based on a cylinder around the solute lead to size-independent PMFs, down to systems of only 16 lipids per monolayer. In summary, compared to popular setups that simulate a single solute in a membrane of 128 lipids with a Lennard-Jones cutoff of 1.2 nm, the measures applied here yield a speedup in sampling by factor of ~40, without reducing the accuracy of the calculated PMF. *Published by AIP Publishing.* [http://dx.doi.org/10.1063/1.4963192]

I. INTRODUCTION

Passive diffusion over the lipid membrane is a common mechanism for drugs to enter the cell, making low membrane permeability the reason for failure of a significant fraction of drug candidates.[1] Hence, in recent years much effort has been invested in the development of computational tools for accurate yet efficient predictions of membrane permeabilities and partition free energies between membranes and water.[2–18] The permeability is mainly determined by the partitioning of the solute into the membrane, which can be quantified by the potential of mean force (PMF) for solute translocation over the membrane. PMFs for membrane permeation are often calculated using molecular dynamics (MD) simulations, which provide an accurate physical model of the membrane (Ref. 7 and references therein). However, MD simulations are not yet used for high-throughput permeability predictions, due to their high computational cost. Hence, computationally efficient setups for such calculations are required, in order to transfer their applicability to pharmaceutical research.

MD-based PMF calculations of membrane permeation require (a) a physical model, defined by the lipid and solutes force fields, the size of the membrane system, and the MD parameters such as cutoffs, thermostats, etc., (b) a reaction coordinate (or order parameter) used to quantify the solute position along the permeation pathway, and (c) a sampling algorithm that ensures sufficient conformational sampling of both the order parameter and orthogonal degrees of freedom. In recent years, much work has been carried out for the development of better force fields for lipids[19–26] and small molecules,[27,28] as well as for improved sampling algorithms to allow for more accurate and more efficient permeation simulations.[8,9,17,18,29,30] In contrast, only few studies systematically analyzed simple methods for accelerating PMF calculations of membrane permeation, such as using smaller simulation systems, shorter cutoffs,[11] or simulating multiple solutes per simulation system, despite the fact that such parameters may be tuned with any MD software without methodological overhead.

In this study, we analyzed the influence of such simple parameters on PMF calculations of membrane permeation, including (a) the system size, given by the number of lipids, (b) the solute-solute distance used when simulating multiple solutes per system, and (c) the cutoffs applied for the calculation of van der Waals interactions, as modeled by the attractive term of the Lennard-Jones (LJ) potential. In addition, to assess the role of the reaction coordinate, we computed PMFs using two different definitions for the membrane center of mass (COM), based either on all lipid atoms or only on the lipid atoms within a cylinder aligned along the membrane normal and centered on the solute. All PMFs were computed using umbrella sampling,[31] but most of the findings reported here are expected to also hold for more sophisticated sampling methods, such as multidimensional metadynamics, simulated tempering, or Hamiltonian replica exchange.[8,9,32,33] Similarly, it is conceivable that some of our findings could be also applicable to other force fields in addition to the united-atom Berger lipid force field[19] used in

[a)]jhub@gwdg.de. URL: http://cmb.bio.uni-goettingen.de/.

our simulations. Overall, we find that the PMF calculations are remarkably robust with respect to membrane size, LJ cutoffs, and solute-solute distance. The artifacts arising with small membranes, short cutoffs, and short solute-solute distances are small compared to the uncertainties due to the force field inaccuracies. In addition, we find that the PMFs are invariant with respect to the membrane size only if the cylinder-based definition for the membrane COM is employed. In contrast, membrane undulations may bias the PMFs if the membrane COM is computed from all lipid atoms.

II. METHODS

A. Simulation setup, parameters, and equilibration

The membrane simulation systems were set up with the MemGen web server (http://memgen.uni-goettingen.de).[34] The systems were composed of 18, 32, 50, 72, 98, or 128 palmitoyl-oleoyl-phosphatidylcholine (POPC) lipids, plus 50 water molecules per lipid (Fig. 1). For each lipid number, two systems were set up, either with a square or with a hexagonal cross section of the membrane. The energy of each system was minimized using a steepest descent algorithm, and each system was equilibrated for 10 ns. Subsequently, all systems were simulated under equilibrium conditions for 1 μs (18-lipid systems), 600 ns (32-lipid systems), or 290 ns (the rest of the systems). All simulations were conducted with the GROMACS software, version 4.6.[35] During equilibration, the temperature was controlled at 300 K through velocity rescaling[36] (τ = 0.5 ps), and the pressure was kept at 1 bar using a semi-isotropic weak coupling scheme[37] (τ = 1 ps). The

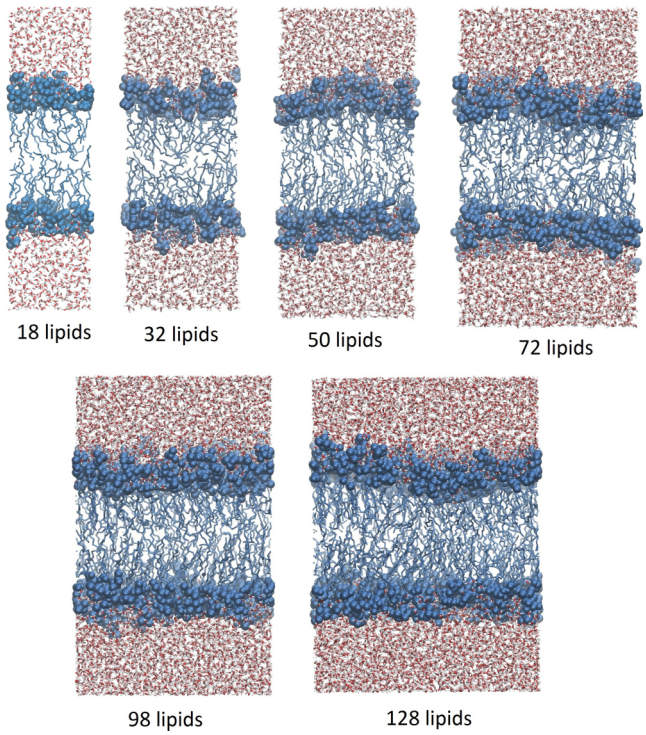

FIG. 1. Lipid membrane systems simulated in this study, containing 18–128 POPC lipids, plus 50 water molecules per lipid. Lipid head groups are shown as blue spheres, tails as blue sticks, and water as sticks colored by atom.

SETTLE[38] algorithm was applied to constrain bond lengths and angles of water molecules, and LINCS[39] was used to constrain all other bond lengths. The integration time step was set to 4 fs. Electrostatic interactions were calculated at every step using the particle-mesh Ewald method,[40,41] with a real-space cutoff of 1 nm, if not stated otherwise. Dispersive interactions were described by a LJ potential with a cutoff of 1 nm, if not stated otherwise. In simulations with shorter LJ cutoffs (see below), the same cutoff was used for the LJ interactions, the direct-space Coulomb interactions, and for neighbor lists. Neighbor lists were updated every 5 steps.

The parameters for POPC were taken from the work of Berger *et al.*[19] with modifications for the oleoyl double bond suggested by Tieleman and Berendsen,[42] and water was described by the SPC model.[43] Non-bonded parameters for ammonia were taken from the OPLS all-atom force field.[44] To make the application of a 4-femtosecond integration time step possible, the ammonia molecules were modeled as rigid. Accordingly, the bonds between the nitrogen atom, the first hydrogen, and the second hydrogen atom were constrained. The third hydrogen atom was constructed as a virtual site. The constraints and the virtual site parameters were chosen such that all N–H bond lengths were constrained to 0.101 nm and all H–N–H angles to 106.4°. The parameters for ibuprofen were taken from the (S)-(+)-ibuprofen model deposited at the Automated Topology Builder (ATB) website,[45] and are based on the Gromos54A7 force field.[46] Methanol parameters were taken from the Gromos43A1 force field.[47] As for ammonia, the angles involving hydrogen atoms were constrained to the equilibrium angle in the ibuprofen and methanol models. Hence, the ammonia, methanol, and ibuprofen models used in this study may be considered as approximate models only. However, as we do not aim to compute accurate absolute PMFs, and we investigate purely the robustness of PMF calculations with respect to various PMF simulation parameters, the used models are sufficient. The deuterium order parameters were computed with the GROMACS module g_order.[35]

B. Umbrella sampling simulations

The umbrella sampling simulations were conducted similarly to previous work.[10,14] Starting structures for the umbrella sampling simulations were randomly chosen from the equilibrium simulations. All PMFs were computed using the membranes with a square cross section. For the PMF calculations with modified LJ cutoffs (see below), the starting structures for umbrella sampling were taken from simulations with a 1.0 nm cutoff, i.e., no additional equilibration with modified LJ cutoffs was conducted. The membrane normal z was chosen as the reaction coordinate for solute permeation, where $z = 0$ corresponds to the COM of the membrane. Here, two different definitions for the membrane COM were employed: (i) The membrane COM was computed from all lipid atoms, denoted henceforth as "all-lipid center of mass" (all-atom COM), or (ii) the membrane COM was computed from a weighted sum over the lipid atoms within a cylinder that was centered at the respective solute and aligned along the z axis. The cylinder was defined by an inner radius R^i_{cyl}

and an outer radius R^o_{cyl}. Atoms within R^i_{cyl} contributed to the COM with a weight of unity, and the weight was linearly switched to zero between R^i_{cyl} and R^o_{cyl}. As shown below, different pairs of (R^i_{cyl}, R^o_{cyl}) were tested in this study. We refer to the latter COM definition as "cylinder-based center of mass" (cylinder-based COM). This reaction coordinate was applied with the GROMACS option "pull-geometry = cylinder."

The reaction coordinate was sampled with an interval $\Delta z_{win} = 0.25$ Å between umbrella windows, and spanned the space from one bulk water regime across the membrane and into the other bulk water regime. The solutes were inserted at the umbrella centers. Ibuprofen was inserted in the *trans* conformation,[9] as downloaded from the ATB website. To save computational resources, multiple umbrella windows were sampled per simulation, while maintaining a distance of ΔZ_{sol} along z between neighboring solutes (illustrated below in Fig. 6(a)). Hence, $N_{sim} = \Delta Z_{sol}/\Delta z_{win}$ simulations were necessary to collect the umbrella histograms over the entire span of the reaction coordinate. The solute-solute distance was set to $\Delta Z_{sol} = 1.5$ nm, if not stated otherwise. Different values for ΔZ_{sol} were tested for ammonia (0.1–2 nm) and ibuprofen (0.75–2.5 nm), in order to test the influence of ΔZ_{sol} on the PMFs. Water molecules that overlapped with the solutes were removed. Overlaps between the solute and lipid atoms were removed by gradually switching on the Lennard-Jones interactions between the solute and the rest of the system within 5000 simulation steps for ibuprofen, and within 150 steps for methanol and ammonia. Only during these insertion simulations a large virtual site atom was added to the center of the aromatic ibuprofen ring, in order to quickly repel the lipid tails from the ring. Subsequently, the energy of each structure was minimized.

A harmonic umbrella potential acting on the COM of the solute was applied (force constant 1000 kJ mol^{-1} nm^{-2}). The umbrella sampling simulations of ibuprofen and methanol were carried out for 50 ns (with exception of the ibuprofen simulations with $\Delta Z_{sol} \leq 1$ nm, which were run for only 20 ns), and the umbrella sampling simulations of ammonia were carried out for 30 ns. The temperature was set to 300 K through a stochastic dynamics integrator ($\tau = 1$ ps).[48] The pressure was controlled at 1 bar using a semi-isotropic weak coupling scheme,[37] while scaling the box in the x-y plane only, and keeping the box dimension in the z-direction fixed.

C. Construction of PMFs

After removing the first 10 ns for equilibration, the PMFs were computed with the weighted histogram analysis method (WHAM),[49] as implemented in the g_wham software.[50] Depending on the system, the PMFs were based on 252–330 histograms. Here, the integrated autocorrelation times (IACTs) of the umbrella windows were incorporated in the WHAM iteration procedure as described by Kumar *et al.*[49] IACTs were estimated as described in the g_wham reference,[50] and smoothed along z using a Gaussian filter with $\sigma = 0.2$ nm. First, non-periodic and non-symmetrized PMFs were computed. These PMFs were reasonably symmetric with respect to the membrane center and exhibited only a small offset between the two bulk water regimes, suggesting that the PMFs were reasonably converged. Subsequently, a periodic PMF was computed and symmetrized with respect to the membrane center ($z = 0$), if not stated otherwise. Statistical uncertainties of the PMFs were calculated using the Bayesian bootstrap of complete histograms.[50]

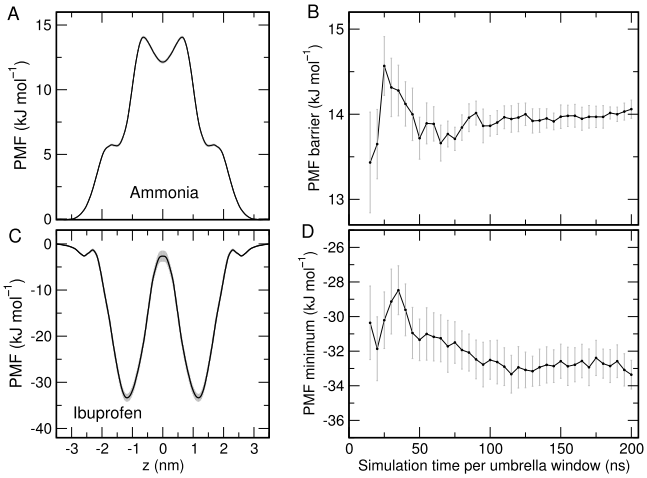

FIG. 2. On the convergence of the PMF calculations: Well-converged PMF for (a) ammonia and (c) ibuprofen based on 200 ns simulations per umbrella window, omitting the first 10 ns of equilibration. (b) Barrier height of ammonia PMF and (d) depth of ibuprofen PMF well as a function of umbrella sampling simulation time. The error bars computed by bootstrapping (see Sec. II) indicate one SD.

D. Convergence of PMFs

The convergence of the PMFs was investigated using long umbrella simulations of two test cases: (i) ammonia permeation across the 72-lipid patch using $\Delta Z_{sol} = 1$ nm (Figs. 2(a) and 2(b)) and (ii) ibuprofen permeation across the 36-lipid patch using $\Delta Z_{sol} = 1.5$ nm (Figs. 2(c) and 2(d)). The PMFs based on 200 ns of umbrella sampling and the cylinder-based COM definition are presented in Figs. 2(a) and 2(c) for ammonia and ibuprofen, respectively. Figures 2(b) and 2(d) present the barrier height of the ammonia PMF and the minimum depth of the ibuprofen PMF, respectively, versus the umbrella sampling simulation time used to compute the PMF. The curves suggest that the barrier height for ammonia permeation changes less than 1 kJ mol^{-1} if umbrella simulations are extended beyond 30 ns. For ibuprofen, the minimum of the PMF exhibits small drifts in the order of 1–2 kJ mol^{-1} if the simulations are extended beyond 50 ns, possibly reflecting slow adaptations of the membrane to the presence of the ibuprofen solutes.[51] In this study, we restricted the umbrella sampling simulations of ibuprofen to 50 ns to restrict the computational cost. Consequently, the depth of the minima of the ibuprofen PMFs presented here may be systematically underestimated by 1–2 kJ mol^{-1}.

III. RESULTS

A. Effect of the membrane size and the definition of the reaction coordinate

The size of the membrane system could in principle affect the PMFs via three distinct mechanisms. First, increasing the

membrane size allows increased undulations. If the reaction coordinate is taken as the center of mass (COM) distance between the solute and *all* lipid atoms, such undulations may smear out or even completely integrate out the barrier along the permeation pathway.[6] Second, finite size artifacts might influence the lipid structure, thereby also affecting the PMF. Third, interactions of the solute with its periodic images could spuriously stabilize a polar solute inside the lipid membrane.

To test if any of these mechanisms influence the PMF for membrane permeation, we computed the PMFs for permeation of methanol and ibuprofen across membranes with 16, 25, 36, 49, or 64 lipids per monolayer (Fig. 1). Overall, the PMFs reflect the physicochemical properties of methanol and ibuprofen (Fig. 3). The methanol PMFs exhibit a barrier that reflects the polar character of this solute. The barrier height of ~10 kJ mol^{-1} is slightly lower than the experimental water/hexadecane transfer free energy of 15.8 kJ mol^{-1}, possibly due to slight limitations of the force fields applied here.[52] The ibuprofen PMF reasonably agrees with previous studies.[9] The two pronounced minima reflect favorable conformations in which the polar carboxyl group of ibuprofen remains in contact with the polar lipid head groups, while the apolar ibuprofen groups are fully solvated among the apolar lipid tails. These two minima are separated by a barrier at $z = 0$ since transfer of ibuprofen between the two leaflets requires breaking of the favorable carboxyl-head group contacts.

Figures 3(a) and 3(c) demonstrate that the PMFs based on the all-atom COM definition for the membrane exhibit a pronounced dependence on the system size. For methanol, with increasing system size, the barrier decreases and becomes narrower along z, in qualitative agreement with previous simulations of water permeation.[11] For ibuprofen, increasing the system size leads to less pronounced energy wells. Minor deviations from these trends are accounted for by the standard error, which we estimated to be ~0.5 kJ mol^{-1} for the methanol PMFs, and ~1.5 kJ mol^{-1} for the ibuprofen PMFs. The significant effect of the system size, clearly evident in the PMFs computed with the all-atom COM definition, can be readily explained by different degrees of undulation of the membranes.[6,11] For polar solutes, such as methanol, membranes may undulate to avoid solute penetration into the hydrophobic core, leading to lower and narrower barriers (Fig. 3(a)). Likewise, for apolar solutes, such as ibuprofen, the membrane may undulate to keep the solute in the hydrophobic core, leading to less pronounced minima in the PMFs (Fig. 3(c)).

To validate that membrane undulations underlie these trends, we computed PMFs for permeation of the same solutes, but with the cylinder-based COM definition for the membrane. Indeed, with this COM definition, the PMFs from nearly all system sizes agree within the errors (Figs. 3(b) and 3(d)). In order to test the lower limit, we also used an exceptionally small membrane, with only 9 lipids per monolayer, and only then we found small artifacts appearing (black curves). These findings suggest that, even in very small systems of only 16 or 25 lipids per monolayer, finite size artifacts on the membrane structure or interactions of the solute with its periodic images only marginally affect the PMFs. Hence, once the effects of the membrane undulations are removed by using the cylinder-based COM definition, the computed PMFs are independent of the system size, down to 16-25 lipids per monolayer.

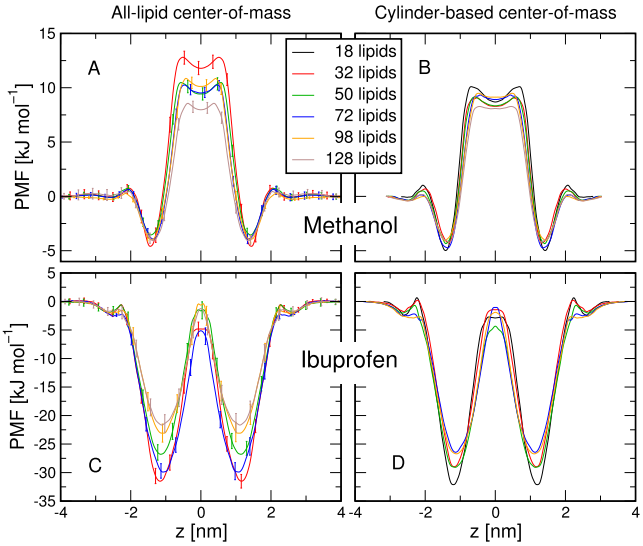

FIG. 3. On the influence of the membrane size on the computed PMFs for methanol ((a) and (b)) and ibuprofen ((c) and (d)) using two different reaction coordinates. The line color encodes the number of lipids per bilayer (see legend). The center of mass (COM) distance between the solute and membrane was computed either using all lipid atoms ((a) and (c)) or using only the lipid atoms within a cylinder whose axis was centered at the solute ((b) and (d)). If all lipid atoms are used for the COM calculations, artifacts due to membrane undulation appear ((a) and (c)). With the cylinder-based coordinate, the PMFs hardly depend on the membrane size ((b) and (d)). Some representative error bars are shown in (a) and (c). Errors in (b) and (d) were ≤0.8 kJ mol^{-1} and ≤1.8 kJ mol^{-1}, respectively, but are not shown for clarity.

1. Structural parameters vs. system size and cross section shape

To rationalize the invariance of the cylinder-based PMFs with respect to the system size, we computed lipid tail order parameters as well as the area per lipid during equilibrium simulations. Figures 4(a) and 4(c) (blue symbols) demonstrate that these structural parameters agreed among nearly all system sizes within the statistical errors. Only the exceptionally small system of 9 lipids per monolayer exhibits visible deviations. Hence, even for small systems down to 16 lipids per monolayer, finite size artifacts seem to hardly bias the membrane structure.

Simulations of globular or membrane proteins were previously conducted in simulation boxes of a hexagonal prism.[54,55] The hexagonal box geometry is motivated from the fact that, at a fixed cross section area, the distance of an atom to its periodic image is larger (by ~7%) as compared to a quadratic cross section area. Hence, membrane simulations using a box of a hexagonal prism might be less prone to finite size artifacts. To test if the box shape may influence the membrane structure, we computed the same structural parameters from equilibrium simulations of systems with number of lipids as before, but using a hexagonal geometry for the simulation box (Figs. 4(b) and 4(c) (red symbols)). As expected, these structural parameters are likewise nearly invariant with respect to the system size. However, a closer

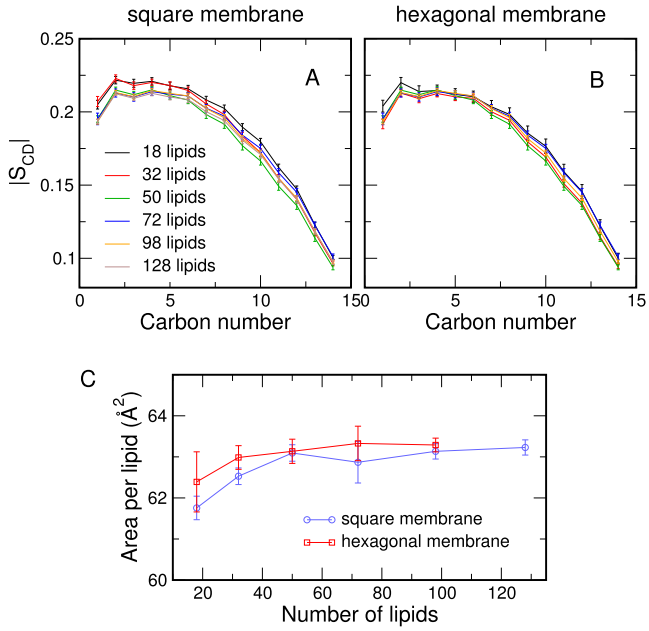

FIG. 4. ((a) and (b)) Deuterium order parameter $|S_{CD}|$ of the saturated palmitoyl tail of POPC, computed from simulations with an increasing number of lipids per bilayer (color code, see legend). $|S_{CD}|$ was computed from simulations with (a) a square membrane cross section or (b) a hexagonal membrane cross section. (c) Area per lipid versus number of lipids in the simulation box. The area per lipid is reported from simulations with a square (blue) or hexagonal (red) cross section. Both reported quantities are nearly invariant with respect to the system size and box shape. Errors denote 1 SD and were computed by block averaging ((a) and (b)) or binning analysis[53] (c).

inspection reveals a slight decrease of the small finite-size artifacts in the hexagonal, as compared to the square membrane patch, visible in the order parameters and the area per lipid at 18 and 32 lipids per bilayer (Figs. 4(a) and 4(b) black/red curves and Fig. 4(c) at ≤32 lipids). Since setting up membranes with a hexagonal cross section is simple with the MemGen web server,[34] and using such a geometry holds no technical disadvantages, a hexagonal simulation box might indeed be advantageous for reducing the finite-size artifacts in systems of ≤32 lipids per bilayer.

2. Cylinder size for cylinder-based center of mass definition

The cylinder-based COM requires the definition of the inner and outer cylinder radii R^i_{cyl} and R^o_{cyl}, between which the weights of the atoms contributing to the COM calculation are switched from unity to zero. Very small radii could in principle lead to artifacts due to computing the COM from only a few lipids. On the other hand, very large radii might allow effects from membrane undulations. To test how the chosen cylinder radii influence the PMFs, we computed PMFs for permeation of methanol using R^i_{cyl}/R^o_{cyl} combinations of 1.0/1.5 nm, 1.4/1.9 nm, and 1.8/2.3 nm, thereby increasing the effective number of lipids inside the cylinder by a factor of ~2.7. As shown in Fig. 5, the size of the cylinder in the tested range has only a marginal effect on the PMFs. Since the smallest cylinder (1.0/1.5 nm) exhibits some minor non-symmetric features, we suggest that radii of around 1.5 or 2 nm provide a suitable choice.

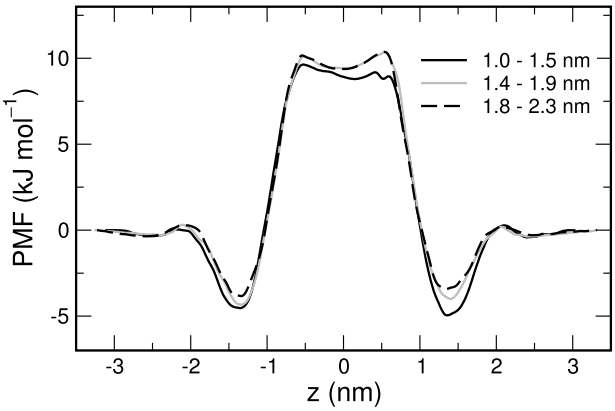

FIG. 5. Non-symmetrized PMFs for permeation of methanol, computed with the cylinder-based reaction coordinate, using different cylinder radii. The inner and outer radii of the cylinders R^i_{cyl} and R^o_{cyl} are indicated in the legend (in nm). In this range, the cylinder radii have only a small influence on the PMFs. Statistical errors (not shown) were ≤0.6 kJ mol^{-1}.

B. Influence of solute-solute distance

A trivial yet efficient method to save computational resources is to collect multiple umbrella histograms per umbrella sampling simulation, by placing multiple solutes into the simulation box.[3,56–58] To this end, the distance between adjacent solutes along the reaction coordinate ΔZ_{sol} should be sufficiently large to avoid significant interactions between the solutes (Fig. 6(a)). Obviously, larger solutes are expected to require a larger ΔZ_{sol} to avoid such solute-solute interactions.

To identify the computationally most efficient setup without artifacts due to solute-solute interactions, we computed the PMFs for ammonia and ibuprofen using a wide range of ΔZ_{sol} between 0.1 and 2.5 nm (Figs. 6(b) and 6(c)). These PMFs were computed with the 72-lipid system (Fig. 1, top right) and using the all-lipid COM definition. The barrier heights from the ammonia PMFs are summarized in Fig. 6(d). For very small $\Delta Z_{sol} \leq 0.75$ nm, we find that the permeation barrier is spuriously reduced, presumably because the polar ammonia solutes stabilize each other in the hydrophobic membrane core. In contrast, for $\Delta Z_{sol} \geq 1.0$ nm all barriers agree within the error, suggesting that $\Delta Z_{sol} = 1.0$ nm provides the computationally most efficient setup for ammonia.

For ibuprofen, PMFs with $\Delta Z_{sol} \leq 1.2$ nm exhibit pronounced artifacts due to solute-solute interactions, since two adjacent ibuprofen solutes may stabilize each other through hydrogen bonds between their carboxyl groups. A typical example is presented in Fig. 6(e), taken from the simulation with $\Delta Z_{sol} = 0.75$ nm. In contrast, using $\Delta Z_{sol} \geq 1.5$ nm leads to similar PMFs, since the ibuprofen molecules are too far from each other to form solute-solute contacts (Fig. 6(f)). Hence, $\Delta Z_{sol} = 1.5$ nm provides the computationally most efficient setup for ibuprofen. Overall, this analysis demonstrates that surprisingly small ΔZ_{sol} values may be used without causing artifacts in the PMFs. For the solutes studied here, collecting multiple umbrella histograms from a single simulation increased the computational efficiency by factors of 9 and 6 for ammonia and ibuprofen, respectively.

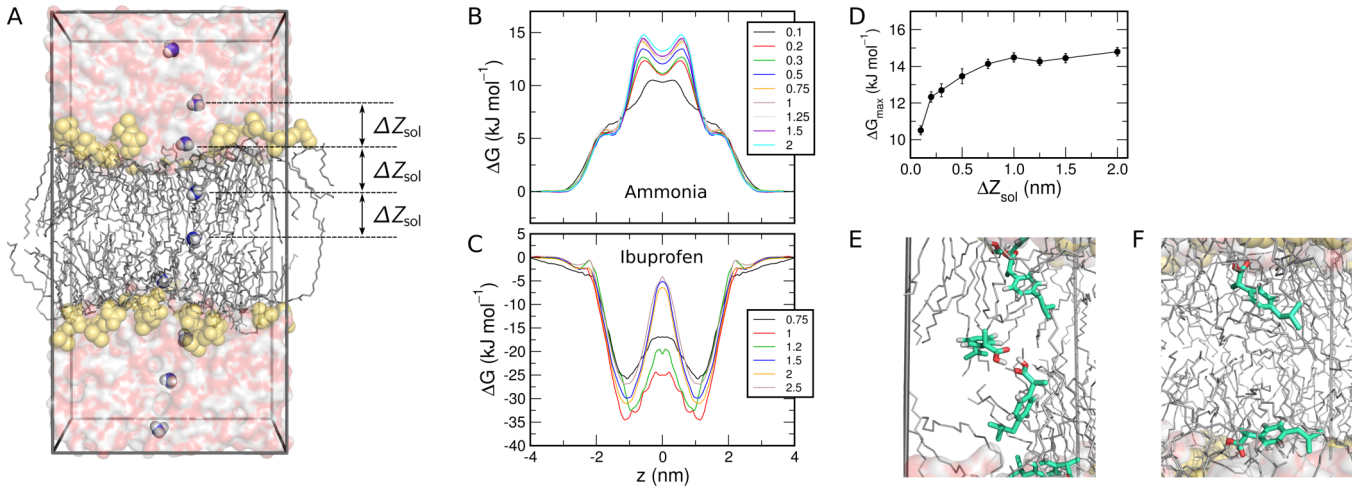

FIG. 6. Influence of the solute-solute distance ΔZ_{sol} along the membrane normal on the computed PMFs $\Delta G(z)$. (a) Typical umbrella sampling simulation system for ammonia permeation, $\Delta Z_{sol} = 1$ nm, containing 72 lipids. (b) PMFs for ammonia and (c) ibuprofen computed using ΔZ_{sol} values between 0.1 nm and 2.5 nm, as indicated in the legends. The ibuprofen PMFs are not affected by ibuprofen-ibuprofen interactions for $\Delta Z_{sol} \geq 1.5$ nm. (d) Barrier height ΔG_{max} of the ammonia PMFs shown in (b) versus ΔZ_{sol}. The ammonia PMFs are not affected by ammonia-ammonia interactions for $\Delta Z_{sol} \geq 1$ nm. (e) and (f) Simulation snapshots from an ibuprofen umbrella sampling simulation using (e) $\Delta Z_{sol} = 0.75$ nm (undesirable interactions between neighboring ibuprofen molecules are evident), and (f) $\Delta Z_{sol} = 1.5$ nm (no major interactions between neighboring ibuprofen molecules are observed).

C. Influence of Lennard-Jones cutoffs

Lennard-Jones (LJ) potential calculations for lipid membrane simulations have been conducted using various cutoff settings, including simple cutoffs, twin-range cutoffs, or switched potentials. Long-range interactions were either ignored or they were modeled using dispersion corrections or Ewald summation.[59] For an excellent overview on common LJ cutoff settings, we refer to the work of Piggot *et al.*[60] It is well established that cutoff settings may influence membrane properties such as order parameters, area per lipid, or diffusion constants.[59–61] In addition, Huang and García reported that short cutoffs enhance the propensity of the Berger force field for forming water defects. For simulations of water permeation, Comer *et al.* found only a small influence of LJ cutoffs on the PMFs, despite a significant effect on the area per lipid.[11]

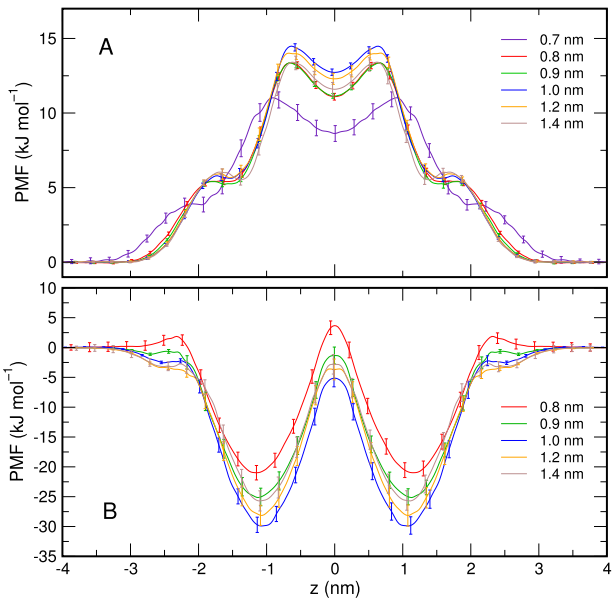

FIG. 7. Influence of the Lennard-Jones and direct-space Coulomb cutoffs on the PMFs for (a) ammonia and (b) ibuprofen. The cutoff is color-coded, see legend. A few representative error bars denoting 1 SD are shown.

Whether LJ cutoffs influence the PMF for permeation of larger drug-like solutes has not been, to our knowledge, systematically addressed. In this study, we computed the PMFs for ammonia and ibuprofen using a wide range of LJ cutoffs between 0.7 and 1.4 nm (Fig. 7). Here, we set ΔZ_{sol} to 1.0 and 1.5 nm for ammonia and ibuprofen, respectively. The ammonia PMFs suggest that, at a cutoff ≥0.8 nm, the main barrier varies at most by 1 kJ mol^{-1}, which is hardly statistically significant (Fig. 7(a)), and is in agreement with the water permeation study by Comer *et al.*[11] Only with a ridiculously short cutoff of 0.7 nm, massive artifacts are observed (Fig. 7(a), indigo). For ibuprofen, the PMFs agree within statistical error when using a cutoff of ≥0.9 nm (Fig. 7(b)). In contrast, using a cutoff of 0.8 nm produces artifacts in the head group region that seem to influence the overall PMF. Hence, with the Berger force field used here, a short cutoff of 0.9 nm seems sufficient for accurate PMF calculations.

We also tested whether dispersion corrections would remove artifacts in the PMFs due to very short cutoffs. To this end, we recomputed the ammonia PMF with a cutoff of 0.7 nm and the ibuprofen PMF with a cutoff at 0.8 nm, while using dispersion corrections for the energy and pressure. Even though applying such corrections altered the PMF curves, the agreement with the PMFs computed with longer cutoffs did not improve (data not shown). Hence, for the PMF calculations considered here, dispersion corrections do not allow for shorter cutoffs, and accordingly more efficient PMF calculations.

IV. DISCUSSION

We have systematically analyzed the influence of various parameters on the accuracy of PMF calculations for membrane permeation of small drug-like molecules. Specifically, we tested the possible effects of the system size, center of mass definition for the reaction coordinate, solute-solute interactions, and LJ cutoffs. Overall, we found that PMF calculations for membrane permeation are remarkably robust. Namely, (i) using small membrane patches, (ii) collecting multiple umbrella histograms from a single simulation, and (iii) using short LJ cutoffs had only a small effect on the computed PMFs. This allows for an increase of the computational efficiency of PMF calculations, by very easy adjustment of these parameters, without losing accuracy. Compared to a standard setup, where a single solute is simulated in a membrane of 128 lipids using a LJ cutoff of 1.2 nm (as often used for simulation of membrane permeation), the methods investigated here may provide a speedup in sampling by a factor of ∼40 or more without causing significant effects on the calculated PMFs.

As a numerical example, a reasonably converged PMF may be computed using umbrella windows separated by 0.25 Å and simulating each window for 50 ns. Using a ΔZ_{sol} = 15 Å, the PMF will require 60 simulations and a total of 3 μs of simulation. On an inexpensive and slightly outdated GPU node with an Nvidia GTX 770 GPU and a 4-core Intel Xeon (E3-1270v2) processor, we achieved ∼500 ns/day for the 32-lipid system using a 0.9 nm cutoff, thus requiring 6 node days per computed PMF. Hence, a rack with 40 such GPU nodes would allow the calculation of ∼2500 PMFs per year. Obviously, these numbers are only an estimate. The simulation time required for convergence varies for different solutes. Solutes larger than ibuprofen require larger ΔZ_{sol} to avoid significant solute-solute interactions. In addition, longer simulations are required to obtain converged PMFs for the permeation across membranes of lipid mixtures, such as membrane models containing cholesterol. Furthermore, the computation time will change with next-generation GPUs. Nevertheless, this back-of-the-envelope calculation demonstrates that accurate high-throughput calculations for membrane permeation of drug-like compounds are within reach.

This study was restricted to hydrophobic or moderately polar solutes that do not form a water defect in the membrane upon permeation. For highly polar solutes, and in particular for ions, most of the findings shown here do not hold. Highly polar or ionic solutes drag water into the membrane and may even form a transmembrane water defect upon permeation.[62–64] We recently showed that the topology of a transmembrane water pore and the pore-closure kinetics may be strongly influenced by finite-size artifacts if too small membrane patches are simulated.[65] In this previous study, we suggested that a patch of at least 128 lipids should be used if transmembrane pores are relevant. Likewise, LJ cutoffs might influence the free-energy landscape of transmembrane pore formation,[61] suggesting that simulations of ion permeation may be influenced by the cutoff. Regarding the solute-solute distance ΔZ_{sol}, if very polar solutes form membrane defects upon permeation, a much larger ΔZ_{sol} will be required to avoid artifacts from solute-solute interactions. However, many uncharged drugs are at most moderately polar, and charged drugs may permeate membranes in a neutral (de)protonated form,[66] suggesting that the findings of this study are applicable to PMF calculations for many drug-like solutes.

We found that varying the LJ cutoff between 1.4 and 0.9 nm has only a small effect on the PMFs computed here. However, modifying cutoff settings should be applied with caution. The cutoff settings are part of the force field and, hence, modifying the cutoff may change various properties of the system. Thus, we cannot exclude that modifying the LJ cutoffs affects the PMFs for solutes not considered here, for instance, by modulation the populations along internal degrees of freedom of the solute. In addition, we cannot exclude that PMF calculations using other lipid force fields are more sensitive with respect to modified LJ cutoffs.

We further tested the influence of the definition of the membrane center of mass (COM), which is used to define the reaction coordinate. When using the all-atom COM definition, we found that the minimum in the PMF for ibuprofen is reduced by up to 10 kJ mol^{-1} when changing the membrane size between 32 and 128 lipids. For methanol, the effect was slightly smaller. In contrast, using the cylinder-based COM definition strongly reduced the influence of the membrane size (Fig. 3), suggesting that the size-dependence of the PMFs was due to membrane undulations. These findings are in line with that of Filipe *et al.* who showed that using the cylinder-based coordinate leads to smaller deformations of the membrane upon permeation.[67] Hence, we recommend the usage of the cylinder-based COM definition in future studies. The radius of the cylinder used to compute the membrane COM seems not to be very critical, but inner and outer radii in the range of 1.5–2 nm seem reasonable (Fig. 5).

In this study, we carried out straightforward umbrella sampling simulations, which are technically simple and are implemented in many MD packages. Since such simulations parallelize trivially, that is, they do not require any communication between the individual simulations, the setup is robust for (worldwide) distributed computing platforms, and the simulations will scale with the rapidly increasing number of CPU and GPU cores. These properties make umbrella sampling an attractive MD setup. Nevertheless, many of the conclusions drawn here for umbrella sampling hold also for more sophisticated sampling algorithms. For instance, while using umbrella sampling along the membrane normal z, the sampling along orthogonal degrees of freedom (ODFs, such as the solute orientation, or the internal angles of the solute) could be accelerated with metadynamics.[8,9,68] However, during exhaustive sampling of the ODFs, the simulations spend most of the time in states of high free energy that hardly contribute to the PMF along the permeation pathway. Exhaustive sampling of the ODFs may indeed prove important if slow transitions along these degrees of freedom influence the barrier for permeation, as suggested for ibuprofen,[9] but it is far from obvious whether it generally yields faster convergence of the PMF. Alternatively, metadynamics may be used to first identify a good reaction coordinate, along which the PMF is afterwards computed with umbrella sampling.[29]

Other work in this field has focused on accelerating the sampling along the main reaction coordinate.[30,32] However, to our knowledge, none of these approaches have been used with multiple solutes along the membrane normal. For instance, Neale *et al.* used replica-exchange Monte-Carlo moves between adjacent umbrella windows; however, this strategy requires a communication between the individual umbrella sampling simulations.[32] Likewise, metadynamics has been successfully used to compute a PMF for membrane permeation. In a setup with a single solute per simulation system (i.e., an infinitely large ΔZ_{sol}), metadynamics yielded a PMF with slightly smaller error bars as compared to umbrella sampling, suggesting that metadynamics may distribute the sampling very efficiently along the reaction coordinate.[30] However, it remains to be shown whether this advantage outweighs (i) the increased sampling from simulating multiple umbrella windows per simulation (i.e., using a finite ΔZ_{sol}) and (ii) the practical benefits due to the trivial parallelization of umbrella sampling. We believe that additional work will be required to identify the computationally best sampling algorithm for computing PMFs for membrane permeation. By focusing on simple parameters such as membrane size, cutoffs, solute-solute distance, and COM definition, the present study complements ongoing algorithmic developments and may guide the search for efficient computational methods to study membrane permeation.

ACKNOWLEDGMENTS

We thank Igor Ariz for technical support with the umbrella sampling simulations and Neha Awasthi for critically reading the manuscript. Financial support through the Deutsche Forschungsgemeinschaft (Grant No. HU 1971-1/1) is gratefully acknowledged.

[1]C. A. Lipinski, "Avoiding investment in doomed drugs," Curr. Drug Discovery **1**, 17–19 (2001).
[2]S. J. Marrink and H. J. C. Berendsen, "Permeation process of small molecules across lipid membranes studied by molecular dynamics simulations," J. Phys. Chem. **100**, 16729–16738 (1996).
[3]D. Bemporad and J. W. Essex, "Permeation of small molecules through a lipid bilayer: A computer simulation study," J. Phys. Chem. B **108**, 4875–4884 (2004).
[4]J. L. MacCallum and D. P. Tieleman, "Interactions between small molecules and lipid bilayers," Curr. Top. Membr. **60**, 227–256 (2008).
[5]M. Orsi, W. E. Sanderson, and J. W. Essex, "Permeability of small molecules through a lipid bilayer: A multiscale simulation study," J. Phys. Chem. B **113**, 12019–12029 (2009).
[6]C. Neale and R. Pomès, "Sampling errors in free energy simulations of small molecules in lipid bilayers," Biochim. Biophys. Acta, Biomembr. **1858**, 2539 (2016).
[7]E. Awoonor-Williams and C. N. Rowley, "Molecular simulation of nonfacilitated membrane permeation," Biochim. Biophys. Acta, Biomembr. **1858**, 1672–1687 (2016).
[8]Z. Ghaemi, M. Minozzi, P. Carloni, and A. Laio, "A novel approach to the investigation of passive molecular permeation through lipid bilayers from atomistic simulations," J. Phys. Chem. B **116**, 8714–8721 (2012).
[9]J. P. M. Jämbeck and A. P. Lyubartsev, "Exploring the free energy landscape of solutes embedded in lipid bilayers," J. Phys. Chem. Lett. **4**, 1781–1787 (2013).
[10]F. Zocher, D. van der Spoel, P. Pohl, and J. S. Hub, "Local micro-partition coefficients govern solute permeability of cholesterol-containing membranes," Biophys. J. **105**, 2760–2770 (2013).
[11]J. Comer, K. Schulten, and C. Chipot, "Calculation of lipid-bilayer permeabilities using an average force," J. Chem. Theory Comput. **10**, 554–564 (2014).
[12]J. Comer, K. Schulten, and C. Chipot, "Diffusive models of membrane permeation with explicit orientational freedom," J. Chem. Theory Comput. **10**, 2710–2718 (2014).
[13]S. Jakobtorweihen, A. C. Zuniga, T. Ingram, T. Gerlach, F. Keil, and I. Smirnova, "Predicting solute partitioning in lipid bilayers: Free energies and partition coefficients from molecular dynamics simulations and cosmomic," J. Chem. Phys. **141**, 045102 (2014).
[14]C. Wennberg, D. van der Spoel, and J. S. Hub, "Large influence of cholesterol on solute partitioning into lipid membranes," J. Am. Chem. Soc. **134**, 5351–5361 (2012).
[15]V. V. Galassi and G. M. Arantes, "Partition, orientation and mobility of ubiquinones in a lipid bilayer," Biochim. Biophys. Acta, Biomembr. **1847**, 1560–1573 (2015).
[16]L. W. Votapka, C. T. Lee, and R. E. Amaro, "Two relations to estimate membrane permeability using milestoning," J. Phys. Chem. B **120**, 8606–8616 (2016).
[17]C. T. Lee, J. Comer, C. Herndon, N. Leung, A. Pavlova, R. V. Swift, C. Tung, C. N. Rowley, R. E. Amaro, C. Chipot, Y. Wang, and J. C. Gumbart, "Simulation-based approaches for determining membrane permeability of small compounds," J. Chem. Inf. Model. **56**, 721–733 (2016).
[18]C. Lv, E. W. Aitchison, D. Wu, L. Zheng, X. Cheng, and W. Yang, "Comparative exploration of hydrogen sulfide and water transmembrane free energy surfaces via orthogonal space tempering free energy sampling," J. Comput. Chem. **37**, 567–574 (2016).
[19]O. Berger, O. Edholm, and F. Jähnig, "Molecular dynamics simulations of a fluid bilayer of dipalmitoylphosphatidylcholine at full hydration, constant pressure, and constant temperature," Biophys. J. **72**, 2002–2013 (1997).
[20]S.-W. Chiu, S. A. Pandit, H. Scott, and E. Jakobsson, "An improved united atom force field for simulation of mixed lipid bilayers," J. Phys. Chem. B **113**, 2748–2763 (2009).
[21]J. P. Ulmschneider and M. B. Ulmschneider, "United atom lipid parameters for combination with the optimized potentials for liquid simulations all-atom force field," J. Chem. Theory Comput. **5**, 1803–1813 (2009).
[22]T. J. Piggot, D. A. Holdbrook, and S. Khalid, "Electroporation of the E. coli and S. aureus membranes: Molecular dynamics simulations of complex bacterial membranes," J. Phys. Chem. B **115**, 13381–13388 (2011).
[23]J. P. Jämbeck and A. P. Lyubartsev, "Derivation and systematic validation of a refined all-atom force field for phosphatidylcholine lipids," J. Phys. Chem. B **116**, 3164–3179 (2012).
[24]R. Pastor and A. MacKerell, Jr., "Development of the CHARMM force field for lipids," J. Phys. Chem. Lett. **2**, 1526–1532 (2011).
[25]C. J. Dickson, L. Rosso, R. M. Betz, R. C. Walker, and I. R. Gould, "GAFFlipid: A General Amber Force Field for the accurate molecular dynamics simulation of phospholipid," Soft Matter **8**, 9617–9627 (2012).
[26]A. Maciejewski, M. Pasenkiewicz-Gierula, O. Cramariuc, I. Vattulainen, and T. Rog, "Refined OPLS all-atom force field for saturated phosphatidylcholine bilayers at full hydration," J. Phys. Chem. B **118**, 4571–4581 (2014).
[27]K. Vanommeslaeghe, E. Hatcher, C. Acharya, S. Kundu, S. Zhong, J. Shim, E. Darian, O. Guvench, P. Lopes, I. Vorobyov, and A. D. MacKerell, Jr., "CHARMM general force field: A force field for drug-like molecules compatible with the CHARMM all-atom additive biological force fields," J. Comput. Chem. **31**, 671–690 (2010).
[28]J. Wang, R. M. Wolf, J. W. Caldwell, P. A. Kollman, and D. A. Case, "Development and testing of a general amber force field.," J. Comput. Chem. **25**, 1157–1174 (2004).
[29]Y. Zhang and G. A. Voth, "Combined metadynamics and umbrella sampling method for the calculation of ion permeation free energy profiles," J. Chem. Theory Comput. **7**, 2277–2283 (2011).
[30]D. Bochicchio, E. Panizon, R. Ferrando, L. Monticelli, and G. Rossi, "Calculating the free energy of transfer of small solutes into a model lipid membrane: Comparison between metadynamics and umbrella sampling," J. Chem. Phys. **143**, 144108 (2015).
[31]G. M. Torrie and J. P. Valleau, "Monte Carlo free energy estimates using non-Boltzmann sampling: Application to the sub-critical Lennard-Jones fluid," Chem. Phys. Lett. **28**, 578–581 (1974).
[32]C. Neale, C. Madill, S. Rauscher, and R. Pomès, "Accelerating convergence in molecular dynamics simulations of solutes in lipid membranes by conducting a random walk along the bilayer normal," J. Chem. Theory Comput. **9**, 3686–3703 (2013).
[33]K. Huang and A. E. García, "Acceleration of lateral equilibration in mixed lipid bilayers using replica exchange with solute tempering," J. Chem. Theory Comput. **10**, 4264–4272 (2014).
[34]C. J. Knight and J. S. Hub, "MemGen: A general web server for the setup of lipid membrane simulation systems," Bioinformatics **31**, 2897–2899 (2015).

[35]S. Pronk, S. Páll, R. Schulz, P. Larsson, P. Bjelkmar, R. Apostolov, M. R. Shirts, J. C. Smith, P. M. Kasson, D. van der Spoel, B. Hess, and E. Lindahl, "GROMACS 4.5: A high-throughput and highly parallel open source molecular simulation toolkit," Bioinformatics **29**, 845–854 (2013).
[36]G. Bussi, D. Donadio, and M. Parrinello, "Canonical sampling through velocity rescaling," J. Chem. Phys. **126**, 014101 (2007).
[37]H. J. C. Berendsen, J. P. M. Postma, A. DiNola, and J. R. Haak, "Molecular dynamics with coupling to an external bath," J. Chem. Phys. **81**, 3684–3690 (1984).
[38]S. Miyamoto and P. A. Kollman, "SETTLE: An analytical version of the SHAKE and RATTLE algorithms for rigid water models," J. Comput. Chem. **13**, 952–962 (1992).
[39]B. Hess, C. Kutzner, D. van der Spoel, and E. Lindahl, "Gromacs 4: Algorithms for highly efficient, load-balanced, and scalable molecular simulation," J. Chem. Theory Comput. **4**, 435–447 (2008).
[40]T. Darden, D. York, and L. Pedersen, "Particle mesh Ewald: An N·log(N) method for Ewald sums in large systems," J. Chem. Phys. **98**, 10089–10092 (1993).
[41]U. Essmann, L. Perera, M. L. Berkowitz, T. Darden, H. Lee, and L. G. Pedersen, "A smooth particle mesh ewald potential," J. Chem. Phys. **103**, 8577–8592 (1995).
[42]D. Tieleman and H. Berendsen, "A molecular dynamics study of the pores formed by Escherichia coli ompf porin in a fully hydrated palmitoyloleoylphosphatidylcholine bilayer," Biophys. J. **74**, 2786–2801 (1998).
[43]H. J. C. Berendsen, J. P. M. Postma, W. F. van Gunsteren, and J. Hermans, "Interaction models for water in relation to protein hydration," in *Intermolecular Forces*, edited by B. Pullman (D. Reidel Publishing Company, Dordrecht, 1981), pp. 331–342.
[44]W. L. Jorgensen, D. S. Maxwell, and J. Tirado-Rives, "Development and testing of the OPLS all-atom force field on conformational energetics and properties of organic liquids," J. Am. Chem. Soc. **118**, 11225–11236 (1996).
[45]A. K. Malde, L. Zuo, M. Breeze, M. Stroet, D. Poger, P. C. Nair, C. Oostenbrink, and A. E. Mark, "An automated force field topology builder (ATB) and repository: Version 1.0," J. Chem. Theory Comput. **7**, 4026–4037 (2011).
[46]N. Schmid, A. P. Eichenberger, A. Choutko, S. Riniker, M. Winger, A. E. Mark, and W. F. van Gunsteren, "Definition and testing of the GROMOS force-field versions 54A7 and 54B7," Eur. Biophys. J. **40**, 843–856 (2011).
[47]W. Van Gunsteren, S. Billeter, A. Eising, P. Hünenberger, P. Krüger, A. Mark, W. Scott, and I. Tironi, *Biomolecular Simulation: The GROMOS96 Manual and User Guide* (Biomos b.v., Zürich, Groningen, 1996).
[48]W. F. van Gunsteren and H. J. C. Berendsen, "A leap-frog algorithm for stochastic dynamics," Mol. Simul. **1**, 173–185 (1988).
[49]S. Kumar, D. Bouzida, R. H. Swendsen, P. A. Kollman, and J. M. Rosenberg, "The weighted histogram analysis method for free-energy calculations on biomolecules. I. The method," J. Comput. Chem. **13**, 1011–1021 (1992).
[50]J. S. Hub, B. L. de Groot, and D. van der Spoel, "g_wham–A free weighted histogram analysis implementation including robust error and autocorrelation estimates," J. Chem. Theory Comput. **6**, 3713–3720 (2010).
[51]C. Neale, W. D. Bennett, D. P. Tieleman, and R. Pomès, "Statistical convergence of equilibrium properties in simulations of molecular solutes embedded in lipid bilayers," J. Chem. Theory Comput. **7**, 4175–4188 (2011).
[52]J. Li and P. W. Carr, "Measurement of water-hexadecane partition coefficients by headspace gas chromatography and calculation of limiting activity coefficients in water," Anal. Chem. **65**, 1443–1450 (1993).
[53]B. Hess, "Determining the shear viscosity of model liquids from molecular simulations," J. Chem. Phys. **116**, 209–217 (2002).
[54]S. Vijayakumar, G. Ravishanker, R. Pratt, and D. Beveridge, "Molecular dynamics simulation of a class A β-lactamase: Structural and mechanistic implications," J. Am. Chem. Soc. **117**, 1722–1730 (1995).
[55]J. S. Hub, F. K. Winkler, M. Merrick, and B. L. de Groot, "Potentials of mean force and permeabilities for carbon dioxide, ammonia, and water flux across a Rhesus protein channel and lipid membranes," J. Am. Chem. Soc. **132**, 13251–13263 (2010).
[56]J. S. Hub and B. L. de Groot, "Does CO_2 permeate through Aquaporin-1?," Biophys. J. **91**, 842–848 (2006).
[57]J. L. MacCallum, W. D. Bennett, and D. P. Tieleman, "Distribution of amino acids in a lipid bilayer from computer simulations," Biophys. J. **94**, 3393–3404 (2008).
[58]J. S. Hub and B. L. de Groot, "Mechanism of selectivity in aquaporins and aquaglyceroporins," Proc. Natl. Acad. Sci. U. S. A. **105**, 1198–1203 (2008).
[59]C. L. Wennberg, T. Murtola, B. Hess, and E. Lindahl, "Lennard-jones lattice summation in bilayer simulations has critical effects on surface tension and lipid properties," J. Chem. Theory Comput. **9**, 3527–3537 (2013).
[60]T. J. Piggot, A. Piñiro, and S. Khalid, "Molecular dynamics simulations of phosphatidylcholine membranes: A comparative force field study," J. Chem. Theory Comput. **8**, 4593–4609 (2012).
[61]K. Huang and A. E. García, "Effects of truncating van der Waals interactions in lipid bilayer simulations," J. Chem. Phys. **141**, 105101 (2014).
[62]A. A. Gurtovenko and I. Vattulainen, "Pore formation coupled to ion transport through lipid membranes as induced by transmembrane ionic charge imbalance: Atomistic molecular dynamics study," J. Am. Chem. Soc. **127**, 17570–17571 (2005).
[63]J. L. MacCallum, W. D. Bennett, and D. P. Tieleman, "Transfer of arginine into lipid bilayers is nonadditive," Biophys. J. **101**, 110–117 (2011).
[64]W. D. Bennett and D. P. Tieleman, "The importance of membrane defects lessons from simulations," Acc. Chem. Res. **47**, 2244–2251 (2014).
[65]N. Awasthi and J. S. Hub, "Simulations of pore formation in lipid membranes: Reaction coordinates, convergence, hysteresis, and finite-size effects," J. Chem. Theory Comput. **12**, 3261–3269 (2016).
[66]T. Oruç, S. E. Küçük, and D. Sezer, "Lipid bilayer permeation of aliphatic amine and carboxylic acid drugs: Rates of insertion, translocation and dissociation from md simulations," Phys. Chem. Chem. Phys. **18**, 24511–24525 (2016).
[67]H. A. Filipe, M. J. a. Moreno, T. Róg, I. Vattulainen, and L. M. Loura, "How to tackle the issues in free energy simulations of long amphiphiles interacting with lipid membranes: Convergence and local membrane deformations," J. Phys. Chem. B **118**, 3572–3581 (2014).
[68]Z. Ghaemi, D. Alberga, P. Carloni, A. Laio, and G. Lattanzi, "Permeability coefficients of lipophilic compounds estimated by computer simulations," J. Chem. Theory Comput. **12**, 4093–4099 (2016).